Atomistic molecular dynamics simulation of diffusion in binary liquid *n*-alkane mixtures

V. A. Harmandaris
Institute of Chemical Engineering and High Temperature Chemical Processes, ICE/HT-FORTH, GR 26500 Patras, Greece and Department of Chemical Engineering, University of Patras, GR 26500 Patras, Greece

D. Angelopoulou
Department of Physics, University of Patras, GR 26500 Patras, Greece

V. G. Mavrantzas
Institute of Chemical Engineering and High Temperature Chemical Processes, ICE/HT-FORTH, GR 26500 Patras, Greece

D. N. Theodorou[a)]
Institute of Chemical Engineering and High Temperature Chemical Processes, ICE/HT-FORTH, GR 26500 Patras, Greece and Department of Chemical Engineering, University of Patras, GR 26500 Patras, Greece

(Received 10 December 2001; accepted 7 February 2002)

Well relaxed atomistic configurations of binary liquid mixtures of *n*-alkanes, obtained via a new Monte Carlo simulation algorithm [Zervopoulou *et al.*, J. Chem. Phys. **115**, 2860 (2001)], have been subjected to detailed molecular dynamics simulations in the canonical ensemble. Four different binary systems have been simulated (C_5-C_{78} at $T=474$ K, $C_{10}-C_{78}$ at $T=458$ K, and $C_{12}-C_{60}$ at $T=403.5$ and 473.5 K). Results are presented for the diffusion properties of these mixtures over a range of concentrations of the solvent (lighter component). The self-diffusion coefficients of the *n*-alkanes, calculated directly from the simulations, are reported and compared with the predictions of two theories: the detailed free volume theory proposed by Vrentas and Duda based on the availability of free volume in the blends, and a combined Rouse diffusant and chain-end free volume theory proposed by Bueche and von Meerwall *et al.* A direct comparison with recently obtained experimental data [von Meerwall *et al.*, J. Chem. Phys. **111**, 750 (1999)] is also presented. © *2002 American Institute of Physics.* [DOI: 10.1063/1.1466472]

I. INTRODUCTION

The diffusivity of small molecular species dissolved in rubbery polymers is an important dynamic property. The mobility of small molecules in macromolecular materials dictates the effectiveness of polymerization reactors operating under conditions of partial or full diffusion control, as well as the physical and chemical characteristics of the polymer produced. Molecular weight distribution and average molecular weight, for example, are among the physical properties influenced by the diffusion-controlled termination step of free radical polymerization reactions. In addition, molecular transport affects the mixing of plasticizers with polymers, the removal of residual monomer or solvent from polymers through devolatilization processes, and the formation of films, coatings, and foams from polymer–solvent mixtures.

From the point of view of theoretical developments, the most successful theory for describing molecular diffusion of penetrants in polymer-penetrant systems is the free volume theory proposed by Vrentas and Duda.[1–8] This theory is based on the assumption of Cohen and Turnbull[3] that molecular transport relies on the continuous redistribution of free volume elements within the liquid. The availability of free volume within the system controls molecular transport. This model describes mass transfer in solutions consisting of long polymer chains mixed with small solvent molecules both above and below T_g. Through a careful estimation of the adjustable parameters, the theory can be applied to a wide variety of systems of different concentrations, temperatures, and molecular weights.

The basic principles of the free volume theory have been used extensively by many researchers in order to study diffusion of oligomer probes or solvents in polymer matrices, melts, or solutions. Using nuclear magnetic resonance (NMR), Waggoner *et al.*[9] measured the self-diffusion coefficients of several solvents in different polymers at polymer concentrations ranging from 0 to 50 wt % at 25 °C, and reported very good agreement with the free-volume approach, mainly at higher polymer concentrations.

Building on the ideas of free volume theory, von Meerwall *et al.*[10–12] proposed a combined theory for the diffusion of *n*-alkanes and binary blends, based on the notions of monomeric friction coefficient, intrinsic thermal activation, and host free volume effects, with particular attention to the chain-end contribution.[13] To test their theory, they employed the pulsed-gradient spin-echo (PGSE) NMR method to measure the self-diffusion coefficient D in a series of monodis-

a)Electronic mail: doros@sequoia.chemeng.upatras.gr

perse *n*-alkane liquids and *cis*-1,4 polyisoprene (PI) melts, as well as in binary alkane–polymer blends, over the full concentration range of the *n*-alkanes, at various temperatures. By proper fitting of the densities and diffusivities of the monodisperse *n*-alkanes, they extracted values for the parameters needed in the theory to predict the diffusion coefficients. The combined theory was seen to reproduce the experimental data for the diffusion coefficients of both components in the binary blends at least semiquantitatively, in the entire concentration range of the solvent component.[11]

In an earlier article we studied the self-diffusion coefficients of chains in polydisperse polymer melts of mean chain length ranging from C_{24} to C_{150} with atomistic molecular dynamics (MD) simulations and compared our results with the Rouse model.[14] The study has been extended into the regime of entangled polymer melts of length up to C_{250} and the results have been compared against the predictions of the Rouse and reptation theories.[15] More recently, we have extended the study of self-diffusion to strictly monodisperse *n*-alkane and *cis*-1,4 PI liquids, where we compared the results of atomistic MD simulations with the predictions of the combined Rouse diffusion and chain end free volume theory proposed by von Meerwall *et al.*[16] In the present work we extend the latter study to binary liquid *n*-alkane blends. The main objective of this paper is to compare the results of our MD simulations for the self-diffusion in the binary systems with the predictions of the free volume theory proposed by Vrentas and Duda[2] and the combined chain end free volume theory proposed by Bueche[13] and von Meerwall.[10] Key to this approach is a novel Monte Carlo (MC) method developed lately[17] for the prediction of sorption equilibria of oligomers in polymer melts, which allows collecting well-equilibrated configurations of binary mixtures of the desired composition. The binary *n*-alkane configurations obtained from this MC method are subjected to MD simulations for the subsequent study of their diffusion properties.

The paper is organized as follows: Section II presents the molecular model used in the present work, outlines the basic characteristics of the MD algorithm employed in the simulation, and gives a complete account of the mixtures studied. Section III reviews the basic assumptions and the most important equations of the free volume theory proposed by Vrentas and Duda and the combined Rouse and chain end free volume theory presented by Bueche and von Meerwall. Results from the MD simulations conducted in the course of this work and a detailed comparison with the predictions of the two theories and with available experimental data are presented in Sec. IV. Finally, Sec. V summarizes the major conclusions and presents plans for future work.

II. MOLECULAR MODEL: METHODOLOGY AND SYSTEMS STUDIED

A united-atom description is used in the present work, with each methylene and methyl group modeled as a single Lennard-Jones (LJ) interacting site. Site–site intra- and intermolecular interactions are defined according to the NERD model.[18] Nonbonded interactions are described by a Lennard-Jones potential of the form

$$U_{\mathrm{LJ}}(r)=4\epsilon\left[\left(\frac{\sigma}{r}\right)^{12}-\left(\frac{\sigma}{r}\right)^{6}\right] \tag{1}$$

with $\epsilon=0.091$ kcal/mol and $\sigma=3.93$ Å for the CH_2-CH_2 interaction, and $\epsilon=0.207$ kcal/mol and $\sigma=3.91$ Å for the CH_3-CH_3 interaction. The CH_2-CH_3 interaction parameters are determined by the Lorentz–Berthelot rules through

$$\epsilon_{CH_2-CH_3}=\sqrt{\epsilon_{CH_2}\epsilon_{CH_3}},\quad \sigma_{CH_2-CH_3}=\frac{\sigma_{CH_3}+\sigma_{CH_2}}{2}. \tag{2}$$

The LJ potential describes all intermolecular site–site interactions as well as intramolecular interactions between sites separated by more than three bonds.

A bond-bending potential of the form

$$U_b=\frac{k_\theta}{2}(\theta-\theta_0)^2 \tag{3}$$

is also used for every skeletal bond angle θ, with $k_\theta=124.1875\,\mathrm{kcal\,mol^{-1}\,rad^{-2}}$ and $\theta_0=114°$.

Associated with each dihedral angle φ is a torsional potential of the form

$$U_t=c_0(1+\cos\phi)+c_1(1-\cos 2\varphi)+c_2(1+\cos 3\phi) \tag{4}$$

with $c_0=0.7054$, $c_1=-0.1355$, and $c_2=1.5724$ in kcal/mol.

Adjacent methyl and methylene groups along each chain backbone are maintained at a fixed distance $l=1.54$ Å from each other using the SHAKE method.[19,20]

The equations of motion are integrated with a velocity Verlet method. As explained in detail in a recent article,[16] to speed-up the MD simulations a multiple time step algorithm is employed in our simulations, the reversible reference system propagator algorithm (rRESPA), first proposed by Tuckerman *et al.*[21,22] In all simulations reported in the present study, the smaller time step dt has been taken equal to 1 fs and the larger time step Dt equal to $5dt$, i.e., 5 fs. To control the temperature a variation of the rRESPA scheme, the XI-RESPA algorithm that incorporates the Nosé–Hoover thermostat, is used.[22]

The initial well-equilibrated configurations are obtained by a recently introduced novel MC algorithm capable of sampling liquid polymer–oligomer mixture configurations of a variety of compositions, thoroughly relaxed at all length scales.[17] With the implementation of two new MC moves (scission and fusion), this algorithm leads to extremely fast equilibration of the concentration of alkane molecules in the polymer melt and allows predicting the solubility of long oligomers in a polymer matrix over a wide range of fugacities of the oligomers. In the present MD simulations, the volume has always been kept constant at a value corresponding to the mean density of the corresponding system obtained from the MC runs.

In the following discussion, we will denote as 1 and 2 the lighter and the heavier components of the alkane mixture, respectively. Four different liquid *n*-alkane mixtures have been simulated at various values of the weight fraction w_1 of the lighter component. These are as follows.

System 1: A C_5-C_{78} liquid at $T=474\,K$ and $w_1=0.025$, 0.07, 0.16, 0.32, 0.42, 0.52, 0.64, and 0.74, with a polydispersity index of the polymeric C_{78} component $I=1.08$.

System 2: A $C_{10}-C_{78}$ liquid at $T=458\,K$ and $w_1=0.025$, 0.21, 0.25, 0.44, 0.53, 0.63, 0.74, and 0.8, with a polydispersity index of the C_{78} component $I=1.08$.

System 3: A $C_{12}-C_{60}$ liquid at $T=403.5\,K$ for $w_1=0.0$, 0.024, 0.14, 0.2, 0.3, 0.4, 0.5, 0.6, 0.7, 0.8, and 1.0, with a polydispersity index of the C_{60} component $I=1.0$.

System 4: A $C_{12}-C_{60}$ liquid at $T=473.5\,K$ for $w_1=0.0$, 0.024, 0.14, 0.2, 0.3, 0.4, 0.5, 0.6, 0.7, 0.8, and 1.0, with a polydispersity index of the C_{60} component $I=1.0$.

The overall simulation time ranged from 5 to 20 ns, depending on the composition and size of the system studied.

III. THEORY

A. Free volume theory of Vrentas and Duda (Ref. 1)

The free volume theory of transport[1–8] provides a convenient and useful method for predicting and correlating solvent self-diffusion coefficients for polymer–solvent systems. The idea that molecular transport is regulated by free volume was first introduced by Cohen and Turnbull.[3] The diffusion process depends on the probabilities that a molecule will obtain sufficient energy to overcome attractive forces and that a fluctuation in the local density will produce a hole of sufficient size so that the diffusing molecule can jump. According to this picture, the solvent diffusion coefficient, D_1, in a binary mixture may be written as

$$D_1=D_0\exp(-\gamma\overline{V}_1^*/\overline{V}_{FH}), \tag{5}$$

where D_0 is a constant preexponential factor, $\overline{V}_1^*$ is the critical molar free volume required for a jumping unit of component 1 (solvent), $\overline{V}_{FH}$ is the free volume per mole of all individual jumping units in the solution, and γ is an overlap factor, which is introduced because the same free volume is available to more than one jumping unit.

In the original Cohen and Turnbull representation,[3] a jumping unit was envisioned as a single hard-sphere molecule undergoing diffusion. Vrentas and Duda generalized the theory of Cohen and Turnbull to describe motion in binary liquids by using the relationship

$$\overline{V}_{FH}=\frac{\hat{V}_{FH}}{(w_1/M_{1j})+(w_2/M_{2j})}, \tag{6}$$

where $\hat{V}_{FH}$ is the specific hole free volume of a liquid with weight fraction w_i of species i and with jumping unit molecular weights M_{ij}. Combining Eqs. (5) and (6) and introducing an activation energy associated with the fact that a jumping unit must overcome the attractive forces with adjoining molecules prior to a diffusive step, the solvent self-diffusion coefficient D_1 in a rubbery polymer-penetrant mixture can be determined using[5]

$$D_1=D_0\exp\left(-\frac{E}{RT}\right)\exp\left(-\frac{\gamma(w_1\hat{V}_1^*+w_2\xi\hat{V}_2^*)}{\hat{V}_{FH}}\right), \tag{7}$$

$$\frac{\hat{V}_{FH}}{\gamma}=w_1\frac{K_{11}}{\gamma}(K_{21}-T_{g1}+T)+w_2\frac{K_{12}}{\gamma}(K_{22}-T_{g2}+T). \tag{8}$$

In Eqs. (7) and (8), $\hat{V}_i^*$ is the specific hole free volume of component i required for a jump, T_{gi} is the glass transition temperature of component i, and ξ is the ratio of the critical molar volume of the solvent to that of the polymer jumping unit. In addition, E is the energy per mole that a molecule needs in order to overcome the attractive forces which hold it to its neighbors, whereas K_{11} and K_{21} are free volume parameters for the solvent (lighter component) and K_{12} and K_{22} are free volume parameters for the polymer (heavier component).

The concentration dependence of E can be described approximately by considering two energies E_p and E_s, for the polymer and the solvent, respectively. For solvent mass fractions roughly in the range of 0–0.9, E is essentially constant and equal to E_p. As the pure solvent limit is approached, the surroundings of a solvent molecule change and E approaches the value of E_s. In order to avoid unacceptable parameter interaction effects present in applying nonlinear regression analysis, it is necessary to replace the terms containing D_0 and E_s by an average value over the temperature interval of interest:

$$\overline{D}_0\approx D_0\exp\left(-\frac{E_s}{RT}\right). \tag{9}$$

In this case, Eq. (7) becomes

$$D_1=\overline{D}_0\exp\left(-\frac{E^*}{RT}\right)\exp\left(-\frac{\gamma(w_1\hat{V}_1^*+w_2\xi\hat{V}_2^*)}{\hat{V}_{FH}}\right), \tag{10}$$

where

$$E^*=E_p-E_s \tag{11}$$

To evaluate the solvent self-diffusion coefficient D_1, one should first calculate the values of all the parameters appearing in Eqs. (7)–(11). To this end, one can follow the semipredictive method proposed by Vrentas and Vrentas,[5] which consists of the following steps.

(a) The specific hole free volumes $\hat{V}_1^*$ and $\hat{V}_2^*$ are equated to equilibrium liquid volumes at 0 K, which can be determined using methods summarized by Haward.[23]

(b) The parameters K_{12}/γ and $K_{22}-T_{g2}$ can be determined using data for Williams–Landel–Ferry (WLF) constants and the glass transition temperature T_g through the following:

$$\frac{K_{12}}{\gamma}=\frac{\hat{V}_2^*}{2.303(C_1^g)_2(C_2^g)_2}, \tag{12}$$

$$K_{22}-T_{g2}=(C_2^g)_2-T_{g2}, \tag{13}$$

where $(C_1^g)_2$ and $(C_2^g)_2$ are the WLF constants for the polymer.

(c) The quantities $\overline{D}_0$, K_{11}/γ, and $K_{21}-T_{g1}$ can be determined from viscosity–temperature and density–temperature data for the solvent, by performing a nonlinear regression analysis on the expression for the temperature dependence of the viscosity η_1 of the pure solvent:

$$\ln \eta_1 = \ln\left(\frac{0.124\times 10^{-16}\tilde{V}_c^{2/3}RT}{M_1\hat{V}_1^0}\right) - \ln \overline{D}_0 + \frac{\hat{V}_1^*}{(K_{11}/\gamma)(K_{21}+T-T_{g1})}. \quad (14)$$

In Eq. (14), M_1 is the molecular weight of the solvent, $\tilde{V}_c$ is the molar volume of the solvent at its critical temperature, and $\hat{V}_1^0$ is the specific volume of the pure solvent at T.

(d) Finally E^* and ξ are calculated through solvent diffusion data at $w_1=0$, where Eq. (10) takes the form

$$\ln D_1(w_1=0) = \ln \overline{D}_0 - \frac{E^*}{RT} - \frac{\gamma\xi\hat{V}_2^*}{K_{12}(K_{22}+T-T_{g2})}, \quad (15)$$

which can be rearranged to

$$Y = E^* + \xi X,$$

where

$$Y = -RT(\ln D_1 - \ln \overline{D}_0), \quad X = \frac{RT\left(\frac{\gamma\hat{V}_2^*}{K_{12}}\right)}{T+K_{22}-T_{g2}}. \quad (16)$$

With as few as two diffusivity data points, it is possible to construct Y vs X plots using Eqs. (15) and (16). The slope and the intercept of this straight line yield E^* and ξ, respectively. In our work, these two diffusivity data points are obtained directly from the MD simulations for a weight fraction of the solvent component $w_1 \cong 0$.

B. Chain end free volume theory proposed by Bueche and von Meerwall (Refs. 10 and 13)

The chain end free volume theory, first proposed by Bueche,[13] describes how the free volume effects due to molecular chain ends modify the classical Rouse behavior by enhancing D at low M. A combined theory of Rouse diffusant and chain end free volume host effects (BM theory) for monodisperse polymer liquids has been proposed by von Meerwall *et al.*[10] In a more recent work, von Meerwall *et al.*[11] extended the expression used for diffusion in monodisperse melts to describe the two self-diffusion coefficients D_i ($i=1$ or 2) in binary blends of monodisperse polymer liquids as a function of temperature T, the molecular weights M_1 and M_2 of the two components, the volume fraction of the lighter component, v_1, and its fractional free volume, f, as follows:

$$D_i(T,M_1,M_2,v_1) = A\exp(-E_\alpha/RT)M_i^{-1} \times \exp[-B_d/f(T,M_1,M_2,v_1)]. \quad (17)$$

Here, the prefactor A is a constant characterizing the particular polymer, but which is otherwise independent of chain length and/or temperature. As discussed in a recent article,[16] according to this equation, the diffusion coefficient is the product of three terms. The first exponential term describes thermal activation effects with E_α being the thermodynamic activation energy required for the chain end to perform jumps between accessible neighboring sites. The second term (M_i^{-1}) recognizes the Rouse dependence of the diffusivity on the diffusant molecular length or mass. And the third term represents the contribution to the self-diffusion coefficient due to the excess free volume of chain ends. B_d is the volume overlap term; it is a measure of the open volume required for motion of a penetrant molecule or segment relative to the volume of a polymer segment involved in a unit jump process. It is considered to be not far from unity but may depend on the size, shape, and flexibility of the penetrant. Finally $f(T,M_1,M_2,v_1)$ plays the role of a fractional free volume which is highly dependent on T, M_1, M_2, and v_1, the latter being the volume fraction of the lighter component. The value of v_1 is easily related to the measured weight fraction w_1, given the known component densities ρ_i available in literature, through

$$v_1 = \frac{w_1}{w_1 + (1-w_1)\frac{\rho_1}{\rho_2}}. \quad (18)$$

In the absence of entanglements, the familiar Rouse M^{-1} scaling law should apply to each component separately, and thus the two diffusion coefficients in binary *n*-alkane blends should differ across the whole concentration range by a constant factor, the inverse ratio of their molecular weights. The reason for this expected ''ideal'' solution behavior is the universally postulated equal availability of all accessible (hole) free volume to both diffusing components or their motional segments, combined with the absence of any significant volume change of mixing. With these assumptions and by including the dependence of the free volume fraction f on v_1, as proposed by Bueche,[13] we obtain

$$f(T,M_1,M_2,v_1) = f_\infty(T) + 2V_E(T)\rho[T,M^*(v_1)]/M^*(v_1). \quad (19)$$

Equation (19) describes that the dependence of the free volume fraction f should be entirely confined to the chain-end term driven by V_E, the free volume of one mole of chain ends. $f_\infty(T)$ denotes the fractional free volume of the melt at infinite molecular weight, and $1/M^*$ represents a volume-weighted average of the inverse molecular weights of the two components:

$$1/M^*(v_1) = v_1/M_1 + (1-v_1)/M_2. \quad (20)$$

The density ρ can be calculated directly from the specific volume through

$$\rho[T,M_1,M_2,v_1] = [1/\rho_\infty(T) + 2V_E(T)/M^*(v_1)]^{-1}, \quad (21)$$

where $\rho_\infty(T)$ is the melt density at infinite molecular weight.

Equations (17)–(21) are expected to apply in binary unentangled *n*-alkane mixtures. All the parameters needed [i.e., $1/\rho_\infty(T)$, $V_E(T)$, $f_\infty(T)$, A, and E_α] exhibit linear temperature dependencies to a good approximation. von Meerwall *et al.* extracted the above-mentional parameters from fittings to density and self-diffusion of a series of liquid *n*-alkanes from C_8 to C_{60}, and found[10]

$$1/\rho_\infty(T) = [1.142 + 0.000\,76T(^\circ\mathrm{C}) \pm 0.005]\ \mathrm{cm}^3/\mathrm{g}, \quad (22)$$

$$V_E(T) = [13.93 + 0.060T(^\circ\mathrm{C}) \pm 0.3]\ \mathrm{cm}^3/\mathrm{mol}, \quad (23)$$

TABLE I. Predicted values of the chain mean square end-to-end distance $\langle R^2 \rangle$ and of the radius of gyration $\langle R_g^2 \rangle$ for the two components of the $C_{12}-C_{60}$ blend at $T=403$ K, for various weight fractions of C_{12}.

	C_{12}		C_{60}	
w_1	$\langle R^2 \rangle$(Å^2)	$\langle R_g^2 \rangle$(Å^2)	$\langle R^2 \rangle$(Å^2)	$\langle R_g^2 \rangle$(Å^2)
0.2	135±20	16 ±1	1480±100	200±50
0.4	136±15	15.5±1	1450±100	190±40
0.7	136±10	15.5±0.5	1460±100	190±35

$$f_\infty(T)=[0.100+0.0007T(^\circ\mathrm{C})\pm 0.002], \tag{24}$$

$$\langle E_\alpha \rangle = [0.81\pm 0.25] \text{ kcal/mol}, \tag{25}$$

$$A=[0.306\pm 0.009] \text{ cm}^2 \text{ mol/g s}. \tag{26}$$

With these values of the parameters one can predict the diffusion coefficient D_i of component i for a binary blend of n-alkane mixtures over the entire range of concentrations w_i.

IV. RESULTS

Results will be presented concerning the structure and self-diffusion coefficient of liquid binary blends for the four systems simulated as a function of the concentration (weight fraction) of the lighter (solvent) component. The results will be analyzed and compared with the two free volume theories described in Sec. III: the detailed molecular free volume theory proposed by Vrentas and Duda[1] and the theory proposed by Bueche and von Meerwall[10] that combines Rouse diffusion and chain end free volume effects. For the $C_{12}-C_{60}$ systems, the results are also directly compared to the recently published experimental data of von Meerwall *et al.*[11]

A. Structure

At first we check the structural properties of the simulated blends and the dependence of these properties on the concentration of the solvent component, w_1. Table I shows results for the mean square chain end-to-end distance $\langle R^2 \rangle$ and the mean square chain radius of gyration $\langle R_g^2 \rangle$ of the C_{60} and C_{12} alkanes, respectively, in the $C_{12}-C_{60}$ system at $T=403.5$ K for various values of the weight fraction w_1 of C_{12}. It is clear that any effect of w_1 on the dimensions of both C_{12} and C_{60} is below the detection threshold of the simulation. Similarly, w_1 seems to have no effect on the dihedral angle distribution of both C_{12} and C_{60} when C_{12} is dissolved in C_{60}. The same behavior is seen in the other systems simulated and is in agreement with the detailed MC studies of these binary systems.[17]

Direct information about some structural features of the simulated systems can be obtained by inspecting the intermolecular mer–mer pair distribution functions $g(r)$. Figures 1(a)–1(c) show the intermolecular pair distribution functions for the pairs $C_{60}-C_{60}$, $C_{60}-C_{12}$, and $C_{12}-C_{12}$ in $C_{12}-C_{60}$ mixtures of various compositions at $T=403$ K. The intermolecular $g(r)$ for $C_{60}-C_{12}$ seems to exhibit higher values compared to the $C_{60}-C_{60}$ distribution function, especially as regards the first peak. This phenomenon, also seen in the MC study of a C_5-C_{78} system,[17] leads to the conclusion that polymer atoms (or atoms of the heavier component) prefer to be surrounded by atoms of the lighter component rather than by atoms of other polymer chains, proving that C_{12} is a good solvent for C_{60}. As the weight fraction of C_{12} increases, the intermolecular pair distribution function for $C_{60}-C_{60}$ pairs

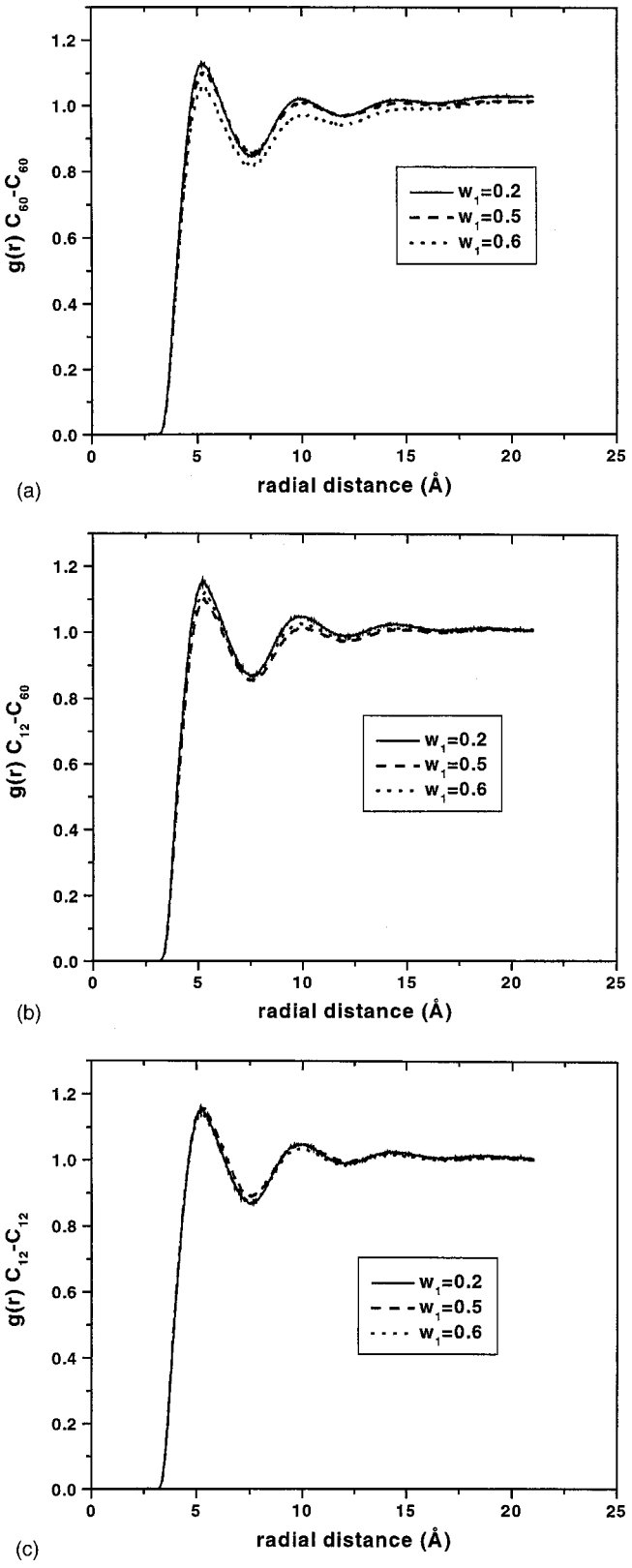

FIG. 1. Intermolecular mer–mer pair distribution function at different C_{12} weight fractions for (a) $C_{60}-C_{60}$, (b) $C_{60}-C_{12}$, and (c) $C_{12}-C_{12}$ pairs, in a $C_{12}-C_{60}$ blend, at $T=403.5$ K.

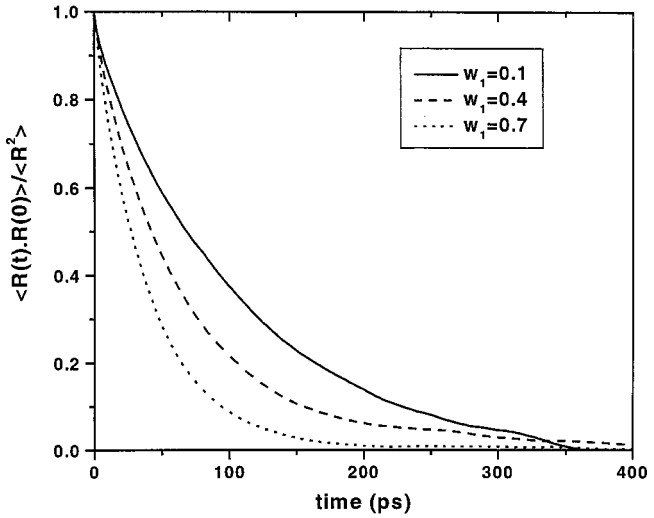

FIG. 2. Autocorrelation function of the end-to-end vector of C_{12} in the binary $C_{12}-C_{60}$ blend at $T=403.5$ K as a function of the weight fraction of C_{12}.

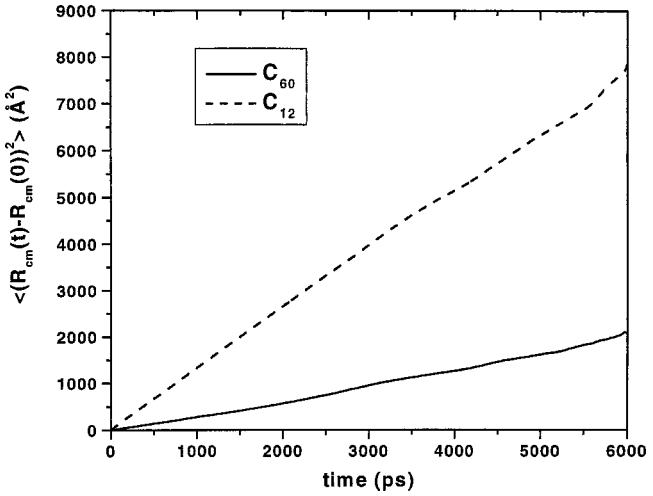

FIG. 3. Mean square displacement of the center of mass of C_{12} and C_{60} molecules as a function of time in a $C_{12}-C_{60}$ blend at $T=403.5$ K ($w_1=0.5$).

falls, indicating that polymer atoms on different chains are more separated from one another, as they are surrounded by more and more oligomer molecules.

Also of interest are the higher values of $g(r)$ for $C_{12}-C_{12}$ pairs compared to $C_{60}-C_{12}$ pairs, which betray a tendency of C_{12} to cluster together, mainly at lower concentrations of C_{12}. This is expected from the form of the Lennard-Jones potential employed in our MD simulations, i.e., the NERD model. In this model, the interaction parameter ϵ is higher for the CH_3 atoms (end segments) than for the CH_2 atoms (middle segments); this end effect is stronger for C_{12} than for C_{60}, where end segments are scarce.

The intermolecular pair distribution functions for the other binary systems (C_5-C_{78} at $T=474$ K, $C_{10}-C_{78}$ at $T=458$ K, and $C_{12}-C_{60}$ at $T=473.5$ K) display the same behavior as described previously. In particular, the end effect phenomenon is stronger in the $C_{10}-C_{10}$ pairs and even stronger in the C_5-C_5 pairs, where chain ends play a more prominent role.

A more detailed report on the structural and conformational properties of the binary *n*-alkane–polymer systems can be found in the previous MC study of the solubility of long alkanes in linear polyethylene.[17]

B. Terminal relaxation: Diffusion

Figure 2 shows the orientational autocorrelation function of the chain end-to-end vector $\langle \mathbf{R}(t)\cdot\mathbf{R}(0)\rangle/\langle R^2\rangle$ for the C_{12} alkane molecules in the $C_{12}-C_{60}$ binary system at $T=403.5$ K, as a function of the weight fraction w_1 of C_{12}. The rate at which $\langle \mathbf{R}(t)\cdot\mathbf{R}(0)\rangle/\langle R^2\rangle$ approaches the zero value is a measure of how fast the chain ''forgets'' its initial configuration. Obviously, as w_1 increases, the autocorrelation function of the C_{12} chain end-to-end vector $\langle \mathbf{R}(t)\cdot\mathbf{R}(0)\rangle/\langle R^2\rangle$ decays faster, i.e., the overall relaxation time of C_{12} decreases. This is expected because as C_{12} is dissolved in the heavier C_{60} component, the total free volume within the system increases due to the additional free volume that the solvent (lighter component) contributes to the mixture. Consequently, the relaxation time of each component in the binary system decreases.

The self-diffusion coefficient D_i of component i ($i=1,2$) of the binary liquid blends simulated here is calculated from the linear part of the mean square displacement of the center of mass of component i as a function of time, $\langle(\mathbf{R}^i_{\text{c.m.}}(t)-\mathbf{R}^i_{\text{c.m.}}(0))^2\rangle$, using the Einstein relation:

$$D_i=\lim_{t\to\infty}\frac{\langle(\mathbf{R}^i_{\text{c.m.}}(t)-\mathbf{R}^i_{\text{c.m.}}(0))^2\rangle}{6t} \tag{27}$$

Figure 3 shows a typical plot of the mean square displacement of the center of mass for the C_{12} and C_{60} components in the $C_{12}-C_{60}$ binary system at $T=403.5$ K for a weight fraction of C_{12}, $w_1=0.5$. From the long-time, linear part of the two curves one can calculate the diffusion coefficients for C_{12} and C_{60} liquids.

Results for the diffusion coefficient of the lighter component (solvent) D_1, for all binary *n*-alkane blends simulated, as a function of the alkane weight fraction w_1, are shown in Figs. 4–7. Also presented in Figs. 4–7 are the predictions from the free volume theory of Vrentas and Duda[1,5] and from the combined theory of Bueche and von Meerwall.[10,13]

To calculate D_1 according to the molecular free volume theory of Vrentas and Duda, we followed the scheme described in steps (a)–(d) of Sec. III A. The viscosity data of the solvent for every system were obtained from the literature.[24–26] A preferable strategy would be to use viscosities computed through MD based on the molecular model invoked in this work. However, the direct MD estimation of viscosity through the Green–Kubo equation, involving the time integral of the autocorrelation function of the instantaneous shear stress, or through the equivalent Einstein expression, is fraught with large numerical error, especially at low temperatures.[14] This is why experimental viscosities were used here for the purpose of comparing against free volume theory. For C_{12}, the experimental viscosity data as a function

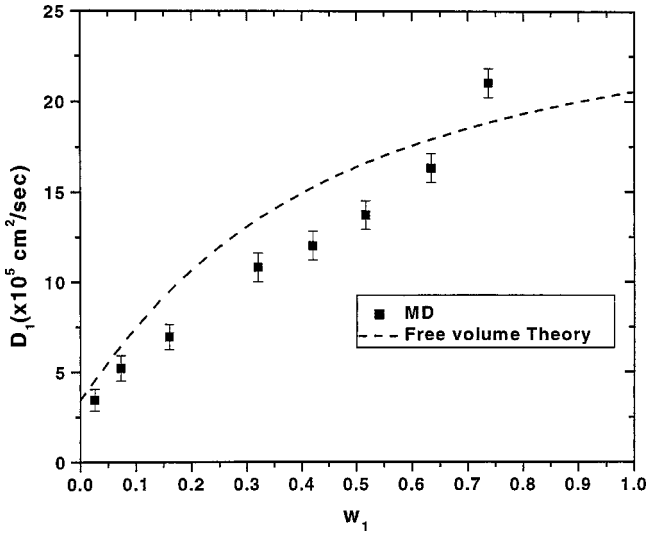

FIG. 4. Self-diffusion coefficient of the C_5 alkane in a C_5-C_{78} system at $T=474$ K and comparison with the predictions of the free volume theory of Vrentas–Duda (dashed line).

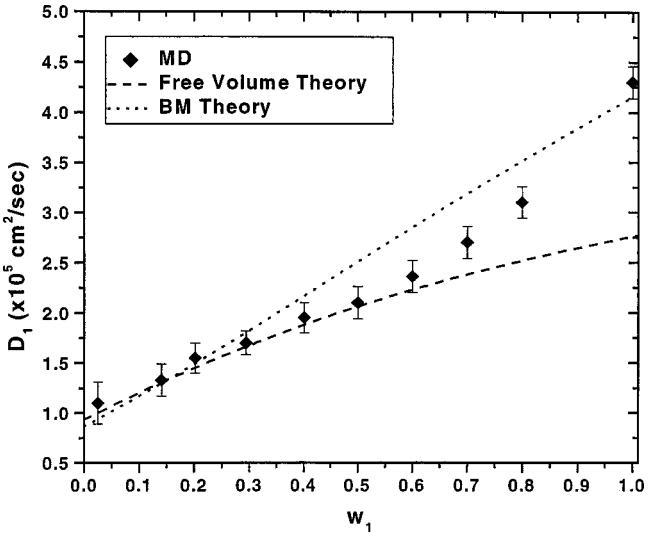

FIG. 6. Self-diffusion coefficient of the C_{12} alkane in a $C_{12}-C_{60}$ system at $T=403.5$ K (circles) and comparison with the predictions of: (a) the free volume theory of Vrentas–Duda (dashed line), and (b) the Bueche–von Meerwall theory (dotted line).

of temperature are shown in Fig. 8 together with the fits of Eq. (14). The two diffusivity data points for the solvent at $w_1 \cong 0$, needed in step (d), were calculated directly from MD simulations with model binary systems containing just a few (up to 3) solvent molecules ($w_1 \cong 0.01$) at two different temperatures for every system, and are shown in Table II. Table III shows in detail the values of all the parameters needed for the evaluation of D_1 for every system simulated.

With the values of the parameters listed in Table III and by using Eqs. (7)–(10), one can predict the solvent diffusion coefficient D_1 for every system studied, as a function of concentration w_1. Predicted values are shown in Figs. 4–7 as dashed lines. The corresponding D_1 values predicted from the chain end free volume theory of Bueche and von Meerwall are shown in Figs. 6 and 7 as dotted lines. The BM values are calculated from Eqs. (17) to (21), with the parameters obtained from fitting the experimental density and diffusion in *n*-alkane melts, Eqs. (22)–(26).

For all binary systems, the self-diffusion coefficient D_i of component i increases as the concentration w_1 of the solvent molecules increases. This can be explained in the same way as the decrease in the relaxation time of each component discussed in conjunction with Fig. 2, i.e., the total free volume increase within the system due to the additional free volume contributed by the solvent component to the mixture in which it is dissolved.

Figure 4 shows how the diffusion coefficient D_1 of C_5 compares with the predictions of the free volume theory for the binary system C_5-C_{78} at $T=474$ K over a range of weight fractions w_1 of C_5. The free volume theory provides a good qualitative description of the simulation results for D_1 up to a concentration of $w_1=0.6$. It is of interest, how-

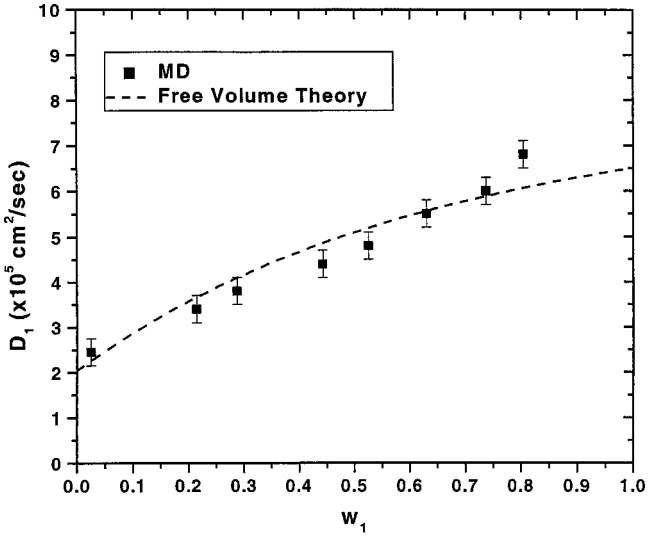

FIG. 5. Same as in Fig. 4 but for the C_{10} alkane in a $C_{10}-C_{78}$ blend at $T=458$ K.

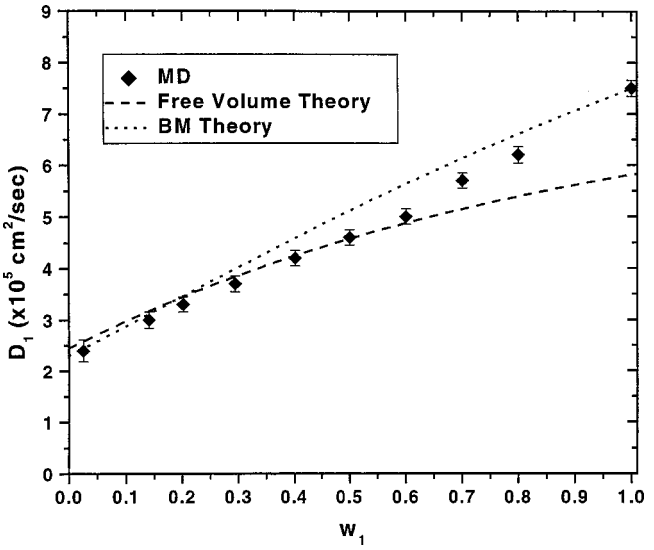

FIG. 7. Same as in Fig. 6 but for a $C_{12}-C_{60}$ system at $T=473.5$ K.

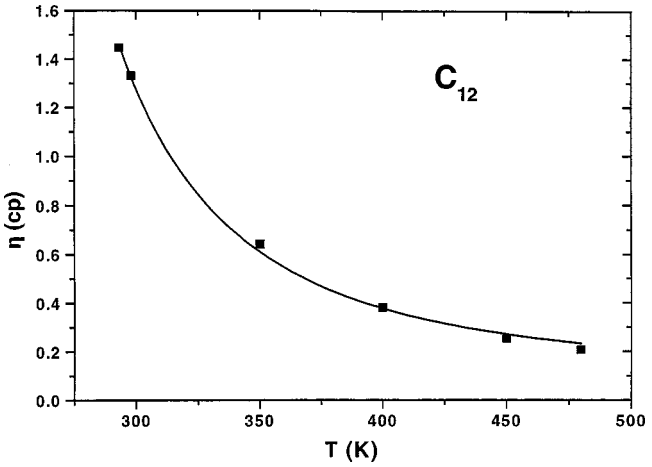

FIG. 8. Viscosity–temperature data for the pure C_{12} used in the calculation of the self-diffusion coefficient of solvent in binary *n*-alkane blends, according to the free volume theory of Vrentas and Duda.

ever, that with a small correction to the preexponential factor D_0 from 1.9 to 1.5×10^{-4} cm^2/s (the value of D_0 that gives the best fit is reported in Table III), excellent quantitative agreement (not shown in Fig. 4) can be established with the simulation results, for concentrations $w_1<0.6$. On the other hand in the high w_1 regime, $w_1>0.6$, the free volume theory seems to underestimate the solvent diffusion coefficient. For the C_5-C_{78}, as well as the $C_{10}-C_{78}$ blend discussed in Fig. 5, no predictions are shown from the Bueche–von Meerwall theory since the components of these systems are outside the range of lengths of the *n*-alkanes (between C_{10} and C_{60}) from which the values of the parameters of the theory, Eqs. (22)–(26), were obtained.[10]

Figure 5 shows results for the diffusion coefficient of C_{10} in the binary system $C_{10}-C_{78}$ at $T=458$ K, and for various values of the weight fraction w_1 of C_{10}. Here again, the free volume theory describes the MD results very well. The agreement is exceptionally good, especially for the smaller weight fractions. As w_1 increases, the predictions of the free volume theory diverge slightly from the results of the MD simulations. This is more obvious for the higher values of the weight fraction of C_{10}, $w_1>0.7$. Again, with a very small adjustment of D_0 in the expression for D_1, Eq. (10) (from 2.0 to 1.9×10^{-4} cm^2/s, results not shown), the agreement between the two sets of data becomes excellent.

Figures 6 and 7 show the self-diffusion coefficient of C_{12} in $C_{12}-C_{60}$ mixtures at $T=403.5$ and 473.5 K, which have been simulated here in the entire range of concentrations of the C_{12} component. For both systems, the simulation results are seen to be very close to the predictions of the free volume theory for concentrations $w_1<0.7$, without any fitting of the preexponential factor D_0. In the high w_1 regime ($w_1>0.7$), the free volume theory seems to underestimate the solvent diffusion coefficient. This is explained by the fact that free volume theory has been developed to describe solvent diffusion in concentrated and semidilute solutions, and is inappropriate for solutions which are very rich in the solvent component (dilute solutions). It is an interesting question how a fully self-consistent application of the free volume theory, employing computed, rather than experimental viscosity data, would affect the comparison with simulation results, especially at high w_1 values. This question will be explored in future work. On the other hand, the Bueche–von Meerwall theory seems to predict the solvent diffusion coefficient D_1 over the entire concentration range semiquantitatively.

TABLE II. MD estimates of alkane self-diffusivities at $w_1\to0$ used for the evaluation of the E^* and ξ parameters in the Vrentas–Duda theory.

	C_5-C_{78}	$C_{10}-C_{78}$	$C_{12}-C_{60}$
T_1 (K)	450	420	403.5
$D_1(T_1)(10^{-5}$ cm^2/mol)	2.1	0.9	1.517
T_2 (K)	474	458	473.5
$D_1(T_2)(10^{-5}$ cm^2/mol)	2.8	2.2	2.28

TABLE III. Values of the parameters used in the calculation of the self-diffusion coefficient of the solvent in binary *n*-alkane mixtures according to the free volume theory of Vrentas and Duda.

	C_5-C_{78} (474 K)	$C_{10}-C_{78}$ (458 K)	$C_{12}-C_{60}$ (403.5 K)	$C_{12}-C_{60}$ (473.5 K)
$\hat{V}_1^*$ (cm^3/g)	1.143	1.041	1.078	1.078
$\hat{V}_2^*$ (cm^3/g)	0.956	0.956	0.959	0.959
$K_{11}/\gamma\,(10^{-3}$ cm^3/g K)	3.0	2.0	1.02	1.02
$K_{21}-T_{g1}$ (K)	−80	−180	−80	−80
$K_{12}/\gamma\,(10^{-4}$ cm^3/g K)	4.61	4.61	4.61	4.61
$K_{22}-T_{g2}$ (K)	−140.9	−140.9	−140.9	−140.9
$D_0\,(10^{-4}$ cm^2/s)	1.9	2.0	9.45	8.85
$D_0\,(10^{-4}$ cm^2/s) (fit)	1.5	1.9	⋯	⋯
E^* (kJ/mol)	−4.0	−3.0	0.8	0.1
ξ	0.45	0.53	0.55	0.57

Values of the self-diffusion coefficient of the polymer component, C_{60}, for the $C_{12}-C_{60}$ systems at the two temperatures studied are shown in Fig. 9. Also presented in Fig. 9 are the results of experimental PGSE NMR measurements

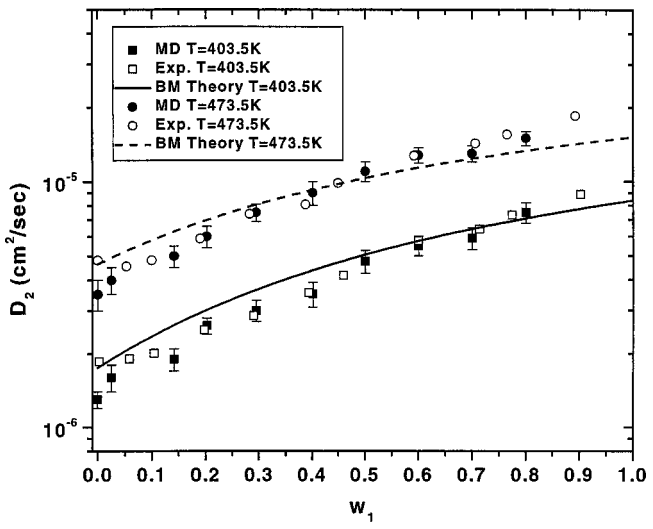

FIG. 9. Predicted diffusion coefficient of the C_{60} molecules in $C_{12}-C_{60}$ blends of various compositions, at $T=403.5$ K (closed squares) and $T=473.5$ K (closed circles), and comparison with experimental data (open symbols). The lines represent the predictions of the Bueche–von Meerwall theory.

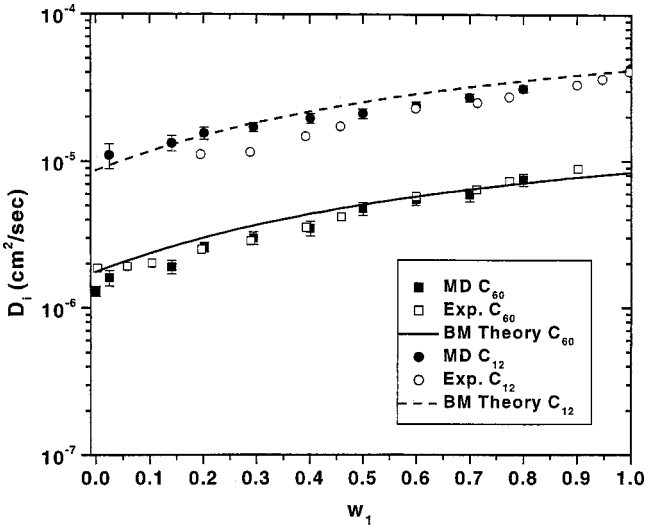

FIG. 10. Diffusion coefficients of the C_{12} and C_{60} molecules in a $C_{12}-C_{60}$ blend at $T=403.5$ K as function of composition w_1, displaying the ''ideal'' solution behavior.

obtained recently by von Meerwall *et al.*[11] for the same blend, as well as the predictions of the Bueche–von Meerwall theory. As stated before, the free volume theory does not predict the diffusivity of the polymer component. The agreement between the MD results and the experimental data is excellent over the entire range of concentration w_1. The Bueche–von Meerwall theory seems to describe the diffusion coefficient of polymer compound very well, especially in the regime of intermediate values of w_1.

The diffusion coefficients of both C_{12} and C_{60} components in the $C_{12}-C_{60}$ system at $T=403.5$ K are shown in Fig. 10. Figure 10 also shows the corresponding experimental values, as well as the predictions of the Bueche–von Meerwall theory. The ratio D_1/D_2 is observed to remain constant over the whole concentration range, exhibiting the ''ideal'' solution behavior which is predicted by the theory.

From all systems simulated, Figs. 5–10, it is obvious that the two theories examined here, i.e., the free volume theory and the Bueche–von Meerwall theory, approach each other very much in the limit of low concentrations of the solvent molecule, w_1. For small and intermediate values of w_1, the free volume theory is seen to be in much better agreement with MD estimates of D_1 than the combined theory. At higher w_1 values, however (i.e., in dilute solutions), the free volume theory becomes unreliable, which should be expected, since it presupposes a sufficient amount of polymer–polymer contact. On the other hand, the combined theory of von Meerwall *et al.*[11] provides both D_1 and D_2 and can cover the entire concentration range, at least semiquantitatively, as it combines concepts from both free volume and dilute solution theories.

V. CONCLUSIONS

Results have been presented from detailed atomistic MD simulations for the diffusion of binary liquid blends of *n*-alkanes and polymers. Four systems have been simulated at various values of the weight fraction of the alkane (solvent) component w_1. The self-diffusivities of the two components have been calculated by applying the Einstein relation. For all systems studied, it was observed that both diffusion coefficients increase when the weight fraction w_1 of solvent increases. This can be attributed to the increase in total free volume due to the additional free volume contributed by the solvent component when it is dissolved in the polymer.

Simulation results have been compared to the predictions of two theories. The first is the free volume theory of Vrentas and Duda,[1] whose parameters were estimated following a semipredictive scheme proposed by Vrentas and Vrentas.[5] This scheme requires experimental viscosity–temperature data for the solvent component, available in the literature, and at least two solvent self-diffusivity data points at different temperatures; the latter were obtained from MD simulations in the limit $w_1 \cong 0$.

Predictions of the free volume theory for the diffusivity were found to be in very good agreement with the MD simulation results only for small and intermediate w_1 values ($w_1 < 0.7$). In the dilute regime ($w_1 > 0.7$), however, the free volume theory significantly underestimates the solvent diffusion coefficient. This should be expected, given that one of the major assumptions of the free volume theory is the presence of a significant amount of polymer molecules in the mixture.

The second theory is the combined Rouse diffusion and chain-end free volume theory of Bueche and von Meerwall,[11,13] designed to describe the diffusion coefficient of both components in a binary liquid system. The parameters needed in applying the theory were taken from regressions of density and diffusion data of a series of monodisperse liquid *n*-alkane systems performed by von Meerwall *et al.*[10] The theory was found to describe MD results for the diffusion of both components over the entire range of concentrations semiquantitatively, particularly for the two $C_{12}-C_{60}$ blends.

The MD simulation results for the diffusion coefficient of components C_{12} and C_{60} in the $C_{12}-C_{60}$ blends at the two different temperatures were further compared with recently obtained experimental data by von Meerwall and collaborators.[11] The agreement was very satisfactory, especially for the range of intermediate concentrations where the experimental measurements are most reliable.

ACKNOWLEDGMENT

One of the authors (D.A.) acknowledges support from the University of Patras, EPEAEK Program on ''Polymer Science and Technology.''

[1] J. L. Duda and J. M. Zielinski, in *Diffusion in Polymers*, edited by P. Neogi (University of Missouri–Rolla Press, Rolla, MO, 1996), Chap. 3, pp. 143–171.
[2] J. S. Vrentas and J. L. Duda, J. Polym. Sci. **15**, 403 (1977); **15**, 417 (1977).
[3] M. H. Cohen and D. Turnbull, J. Chem. Phys. **31**, 1164 (1959).
[4] J. S. Vrentas, C. M. Vrentas, and J. L. Duda, Polym. J. **25**, 99 (1993).
[5] J. S. Vrentas and C. M. Vrentas, Macromolecules **26**, 1277 (1993).
[6] J. C. Vrentas and C. M. Vrentas, Macromolecules **27**, 4684 (1994).
[7] J. C. Vrentas and C. M. Vrentas, Macromolecules **28**, 4740 (1995).

[8] J. C. Vrentas, C. M. Vrentas, and N. Faridi, Macromolecules **29**, 3272 (1996).
[9] R. A. Waggoner, F. D. Blum, and J. M. D. MacElroy, Macromolecules **26**, 6841 (1993).
[10] E. von Meerwall, S. Beckman, J. Jang, and W. L. Mattice, J. Chem. Phys. **108**, 4299 (1998).
[11] E. von Meerwall, E. J. Feick, R. Ozisik, and W. L. Mattice, J. Chem. Phys. **111**, 750 (1999).
[12] E. von Meerwall and R. D. Ferguson, J. Appl. Polym. Sci. **23**, 3657 (1979).
[13] F. Bueche, *Physical Properties of Polymers* (Interscience, New York, 1962).
[14] V. A. Harmandaris, V. G. Mavrantzas, and D. N. Theodorou, Macromolecules **31**, 7934 (1998); **33**, 8062 (2000).
[15] V. A. Harmandaris, V. G. Mavrantzas, D. N. Theodorou, M. Kröger, J. Ramírez, H. C. Öttinger, and D. Vlassopoulos (unpublished).
[16] V. A. Harmandaris, M. Doxastakis, V. G. Mavrantzas, and D. N. Theodorou, J. Chem. Phys. **116**, 436 (2001).
[17] E. Zervopoulou, V. G. Mavrantzas, and D. N. Theodorou, J. Chem. Phys. **115**, 2860 (2001).
[18] S. K. Nath, F. A. Escobedo, and J. J. de Pablo, J. Chem. Phys. **198**, 9905 (1998).
[19] H. C. Andersen, J. Comput. Phys. **52**, 24 (1983).
[20] J. P. Ryckaert, Mol. Phys. **55**, 549 (1985).
[21] M. Tuckerman, B. J. Berne, and G. J. Martyna, J. Chem. Phys. **97**, 1990 (1992).
[22] G. J. Martyna, M. E. Tuckerman, D. J. Tobias, and M. L. Klein, Mol. Phys. **87**, 1117 (1996).
[23] R. N. Haward, J. Macromol. Sci. Rev. Macromol. Chem. C **4**, 191 (1970).
[24] F. A. L. Dullien, AIChE J. **18**, 62 (1972).
[25] P. J. Flory, R. A. Orwoll, and A. Vrij, J. Am. Chem. Soc. **86**, 3507 (1964).
[26] M. Mondello and G. S. Grest, J. Chem. Phys. **22**, 9327 (1997).